# Impact of Finger Placement on the Correlation Properties of Rake Combined Signals

*Konstantinos B. BALTZIS*

RadioCommunications Laboratory, Dept. of Physics, Aristotle University of Thessaloniki, Thessaloniki 541 24, Greece

kmpal@physics.auth.gr

**Abstract.** *3G mobile devices and base stations employ rake receivers. An important issue in the design of such receivers is finger allocation. This paper explores the relationship between finger placement and the correlation properties of rake combined signals. The dependence of correlation coefficients on system parameters such as the multipath characteristics of the propagation channel, the number of users, the processing gain and the thermal noise power is also discussed. Several conclusions useful in the analysis and design of rake receivers are drawn. A low complexity finger placement algorithm is finally suggested. In the proposed receiver, finger allocation is based on the correlation properties of the desired signal component only. The receiver performs close to complex structures in the literature.*

## Keywords

Rake receiver, correlation, spread spectrum, mobile communications, multi-objective optimization.

## 1. Introduction

Direct Sequence Spread Spectrum (DS/SS) is a cost-effective and high quality solution for wireless communications [1], [2]. Among its unique features, the improved multipath resolution achieved by rake diversity significantly increases wireless system performance [1], [3], [4]. Rake diversity improves reception performance by separating multipaths into individual paths for reception and combining. In practice, it reduces the required transmission power and increases system capacity [5].

A rake receiver consists of fingers that collect the resolvable multipaths; each finger can be treated as an independent receiver that composes and demodulates the components of the received signal. After despreading by a local copy of the delayed version of the transmitter's spreading sequence, the signals are suitably combined to perform rake diversity [1], [6]. An important issue in the design of a rake receiver is finger placement. Finger spacing usually equals to the chip period. However, this approach is not a good compromise between performance and complexity. Fractionally spaced reception has gained popularity in the past few years, [7]-[13]. Lately, researchers have analyzed and developed several strategies for the efficient positioning of rake fingers. Typical examples are the maximization of the signal-to-noise ratio of the decision statistic, the minimization of the chip mean square error, the estimation of the strongest multipath components and the simultaneous maximization of received signal power and minimization of correlation between fingers. In most cases, the improved performance of these methods compensates for the increased hardware and/or computational complexity of the receivers.

The main objective of a rake receiver is the optimum combining of the received signals. Their combination is based on the mitigation of thermal noise, interference and multipath effects and an improvement in the signal level of the desired signal. A measure of the received energy and correlation at the fingers of a rake receiver are the correlation coefficients. This paper explores the relationship between the correlation coefficients and finger placement in terms of absolute and relative (i.e. finger spacing) positions. The impact of system parameters such as the power delay profile (PDP) of the propagation channel, the number of active users, the processing gain and the transmission power is also investigated. Finally, the proposal and evaluation of a low computational cost finger placement algorithm assess the merits of the analysis.

The rest of the paper is organized as follows: In Section 2, we discuss the system model. The mathematical formulation that describes the correlation coefficients at the rake fingers is presented in Section 3. Section 4 provides results, applications and discussions. Finally, Section 5 concludes the paper.

## 2. System Model

Let us consider a binary phase shift keying (BPSK) DS/SS communication system with $K$ active users. A unique spreading code sequence is assigned to each user and modulates its binary data sequence such that $N$ continuous chips modulate one information bit at a time. In this case, the processing gain $N$ is the ratio of the bit to the chip period $T_b / T_c$. Without loss of generality, we assume that the signal energy per bit $E_b$ is equal for each user.

Therefore, setting $p(t)$ the normalized chip waveform and $\{b_{k,n}\}$ and $\{c_{k,n}\}$ the data and spreading code sequences of the $k$th user, the equivalent low–pass transmitted signal is

$$x_k(t) = \sqrt{\frac{2E_b}{N}} \sum_{n=-\infty}^{\infty} b_{k,\mathrm{int}(n/N)} c_{k.n}\, p(t - nT_c). \quad (1)$$

The radio channel is modeled as a wide–sense stationary uncorrelated scattering frequency–selective Rayleigh fading one. In this case, the total received signal at the receiver front–end is [14]

$$r(t) = \sum_{k=0}^{K-1} \int_{-\infty}^{\infty} h_k(\tau) x_k(t - \tau_k - \tau)\, d\tau + n(t) \quad (2)$$

where $n(t)$ is a low–pass equivalent process of Additive White Gaussian Noise (AWGN) with double–sided power spectral density $N_0/2$, $\tau_k$ is the time of arrival of the $k$th user's signal and $h_k(t)$ is the channel impulse response of the $k$th user's link. The last is modeled as a complex zero–mean Gaussian random process; its autocorrelation gives the power delay profile $g(t)$ of the channel [6].

Fig. 1 illustrates an $L$-finger rake receiver (it will be mentioned as $L$-rake) model. The received signal $r(t)$ is passed through a tapped delay line with variable (or equal) finger spacing

$$\tau_{i+1,i} = T_{i+1} - T_i,\ i = 1,2..L-1 \quad (3)$$

where $T_i$, $i$=1,2..$L$, are the finger positions. The (optional) additional time delay $T_1$ is introduced at the output of the first correlator through a filter.

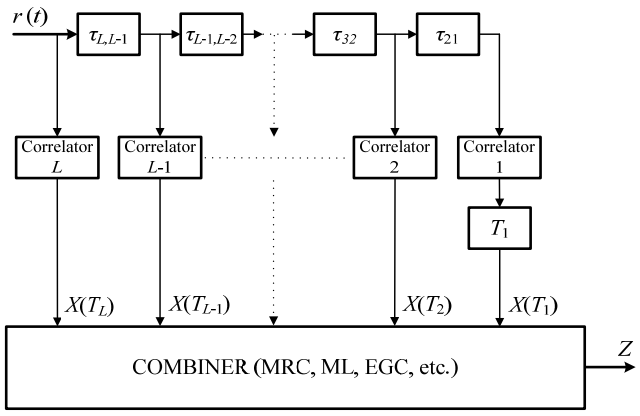


**Fig. 1.** Rake receiver model.

In this structure, the received signal in each finger is despread by passing through a correlator matched to the desired user's spreading sequence. In practice, the output $X(t)$ of the $i$th correlator is identical to the output of a filter matched to the desired user's spreading sequence, sampled at $T_i$, [1], [6], [7]. As a result, $X(t)$ is given by the convolution of $r(t)$ and [7]

$$\upsilon(t) = \frac{1}{\sqrt{N}} \sum_{i=0}^{N-1} c_{0,n}^{*}\, p^{*}(-t - nT_c). \quad (4)$$

The outputs of the fingers are

$$X(t) = X_d(t) + X_k(t) + X_s(t) + X_n(t) \quad (5)$$

where $X_d(t)$, $X_k(t)$, $X_s(t)$, and $X_n(t)$ are the desired user, the multiple user interference (MUI), the intersymbol interference (ISI) and the AWGN signal components, respectively. These are given (under the assumption that the receiver has perfect knowledge of the signal timing of the desired user[1], i.e. $\tau_0 = 0$ ) by the expressions [7]:

$$X_d(t) = \sqrt{2E_b}\, b_{0,1} h_0(t) \otimes R(t), \quad (6)$$

$$X_k(t) = (K-1)\sqrt{2E_b} \sum_{n=-\infty}^{\infty} h_k(t) \otimes d_{k,n} R(t - nT_c - \tau_k), \quad (7)$$

$$X_s(t) = \sqrt{2E_b} \sum_{\substack{n=-\infty \\ n\neq 0}}^{\infty} h_0(t) \otimes d_{0,n} R(t - nT_c), \quad (8)$$

$$X_n(t) = \frac{1}{\sqrt{N}} \sum_{\lambda=0}^{N-1} n(t) \otimes c_{0,\lambda}^{*}\, p^{*}(-t - \lambda T_c) \quad (9)$$

where $\otimes$ denotes the convolution operator, $R(t)$ is the autocorrelation function of the normalized chip waveform and $d_{k,n}$ is the discrete cross-correlation function between the desired and the $k$th user, calculated by

$$d_{k,n} = \frac{1}{N} \sum_{m=0}^{N-1} b_{k,\mathrm{int}[(m+n)/N]} c_{k,m+n} c_{0,m}^{*}. \quad (10)$$

Finally, the signals at the fingers outputs are suitably combined to determine the decision variable $Z$. Combining methods that are commonly used include maximal ratio combining (MRC), maximum likelihood (ML) criterion, equal gain combining (EGC), generalized selection combining (GSC), etc. See, for example, [1], [6]-[8], [11]-[13], [15].

## 3. Mathematical Formulation

The correlation coefficients' matrix **C** of an $L$-rake receiver is an $L$x$L$ Hermitian matrix with elements

$$C_{ij} = \mathrm{E}\left[ X(T_i) X^{*}(T_j) \right],\ i, j = 1,2..L \quad (11)$$

where $\mathrm{E}[X(t_1)X^{*}(t_2)]$ is the correlation function of $X(t)$ conditioned on $b_{1,0}$, [6]-[7]. The diagonal elements denote the autocorrelation at each finger, i.e. the autocorrelation coefficients, and represent the total signal power received at the finger. The rest of the elements are the correlation coefficients between the outputs of two different fingers and give the cross-correlation between these fingers.

Let us consider an $L$-finger rake with its fingers positioned at $\mathbf{T} = (T_1\ T_2\ \ldots\ T_L)$. The correlation coefficients matrix consists of two parts, the desired signal and the noise part, $\mathbf{C}^d$ and $\mathbf{C}^n$, respectively. It is obviously

[1] Time synchronization is achieved by using a known bit sequence that is time multiplexed with the information or transmitted as a separate channel, [1], [5].

$$\mathbf{C} = \mathbf{C}^d + \mathbf{C}^n . \tag{12}$$

Considering that $X_d(t)$, $X_k(t)$, $X_s(t)$, and $X_n(t)$ are generated from independent sources, (5) and (11)-(12) give that the elements of $\mathbf{C}^d$, $\mathbf{C}^n$, and $\mathbf{C}$ are

$$C_{ij}^d = \mathrm{E}\left[ X_d(T_i) X_d^*(T_j) \right], \tag{13}$$

$$C_{ij}^n = \mathrm{E}\left[ X_k(T_i) X_k^*(T_j) \right] + \mathrm{E}\left[ X_s(T_i) X_s^*(T_j) \right] + \\ + \mathrm{E}\left[ X_n(T_i) X_n^*(T_j) \right], \tag{14}$$

$$C_{ij} = C_{ij}^d + C_{ij}^n , \tag{15}$$

respectively. The right terms in (13) and (14) are defined, [7], [11], from the expressions:

$$\mathrm{E}\left[ X_d(T_i) X_d^*(T_j) \right] = 2E_b \times \\ \times \int_{-\infty}^{\infty} g(\tau) R(T_i - \tau) R^*(T_j - \tau) \mathrm{d}\tau , \tag{16}$$

$$\mathrm{E}\left[ X_k(T_i) X_k^*(T_j) \right] = \frac{2E_b(K-1)}{NT_c} \int_{-\infty}^{\infty} R(\tau) R^*(\tau - \tau_{ij}) \mathrm{d}\tau \tag{17}$$

$$\mathrm{E}\left[ X_s(T_i) X_s^*(T_j) \right] = \frac{2E_b}{N} \times \\ \times \left\{ \begin{array}{l} \displaystyle\sum_{\substack{n=-\infty \\ n\neq 0}}^{\infty} \int_{-\infty}^{\infty} g(\tau) R(T_i - \tau - nT_c) R^*(T_j - \tau - nT_c) \mathrm{d}\tau + \\ \displaystyle + \sum_{\substack{n=-N \\ n\neq 0}}^{N} \left( 1 - \frac{|n|}{N} \right) \int_{-\infty}^{\infty} \left[ \begin{array}{l} g(\tau) R(T_i - \tau + nT_c) \times \\ \times R^*(T_j - \tau - nT_c) \end{array} \right] \mathrm{d}\tau \end{array} \right\} , \tag{18}$$

$$\mathrm{E}\left[ X_n(T_i) X_n^*(T_j) \right] = 2N_0 R(\tau_{ij}) \tag{19}$$

where

$$\tau_{ij} \equiv T_i - T_j , \quad i, j = 1, 2..L . \tag{20}$$

This definition is a generalization of (3). Eq. (3) is a special case of (20) for adjacent fingers.

# 4. Results and Discussion

This Section explores the relationship between finger placement and the correlation coefficients of rake combined signals. The impact of channel characteristics, number of users, processing gain and thermal noise is also investigated. Environments with uniform (theoretical assumption) or exponential PDPs, [7], [10], [11], [13], [16]-[18], are considered. For simplicity, time–limited rectangular pulses are assumed (this is a common assumption in DS/SS systems; see, for example, [7], [11], [13], [19], [20]). In the following examples, we set:

$$\rho_X \equiv C_{ij} , \tag{21}$$

$$\rho_{Xd} \equiv C_{ij}^d , \tag{22}$$

$$\rho_{Xm} \equiv \mathrm{E}\left[ X_m(T_i) X_m^*(T_j) \right] \tag{23}$$

where notation $X_m$ stands for $X_k$, $X_s$ and $X_n$.

Expressions (21)-(23) represent the elements of $\mathbf{C}$, $\mathbf{C}^d$ and $\mathbf{C}^n$, respectively. They are, correspondingly, calculated from (11), (16) and (17)-(19). Each term depends on the fingers' positions, but, for presentation simplicity, the $i$ and $j$ indices are omitted in the left terms of (21)-(23). The PDP affects the $\rho_{Xd}$ and $\rho_{Xs}$ coefficients, the processing gain the $\rho_{Xk}$ and $\rho_{Xs}$ while the number of users and AWGN have an impact solely on $\rho_{Xk}$ and $\rho_{Xn}$, respectively.

The section completes with the proposal of a correlation-based finger placement criterion and its application in rake receiver design.

## 4.1 Autocorrelation and Cross-correlation Coefficient Curves

We consider a uniform PDP channel with maximum delay spread $t_{\max}=2T_c$. The remaining system characteristics are $K$=10, $N$=256, and $E_b/N_0$=15dB. Fig. 2 shows the total signal autocorrelation coefficient and the autocorrelation coefficients due to the desired signal and the noise components as a function of finger position. The similarities between $\rho_X$ and $\rho_{Xd}$ curves are evident. Their maxima are at $T_c$. However, $\rho_{Xd}$ is non-zero up to a point; for greater values of $T_i$, the total signal autocorrelation coefficient is only due to noise. This means that the energy gathered from fingers set at distances larger than a point is only due to noise components and explains why rake diversity gain may decrease with the number of fingers, [7], [11]. No clear dependence between noise and $T_i$ is shown.

The MRC rake with fingers spaced at multiple integers of $T_c$ is optimum under the assumption of independent finger signals [21]. However, this assumption is far from reality as it is shown in Fig. 3 and Fig. 4. These figures illustrate the $\rho_X$ and $\rho_{Xd}$ curves for various fingers positions (curve $\tau_{ij} = 0$ shows the autocorrelation coefficient). The similarities between $\rho_X$ and $\rho_{Xd}$ curves are obvious. Notice also, the decrease in their values as $\tau_{ij}$ increases with the only exception of small $T_i$ and $\tau_{ij}$ which is not common in real systems.

In Figs. 5-7, similar illustrations with the ones provided in Figs. 2-4 are given for exponential PDP with decay constant $\tau_d = 2T_C$. The main differences between the uniform and the exponential PDP cases are the absence of a region where coefficients remain almost constant. In addition to that, in the second case, curves are maximized at positions different to $T_c$.

As it has already been mentioned, variations in the PDP have an impact only on the desired signal and the ISI component, (16)-(19). The impact of channel spread on $\rho_X$ and $\rho_{Xd}$ for channels with uniform and exponential PDPs is illustrated in Fig. 8 and Fig. 9, respectively (the impact of PDP on $\rho_{Xs}$ is not presented due to the small contribution

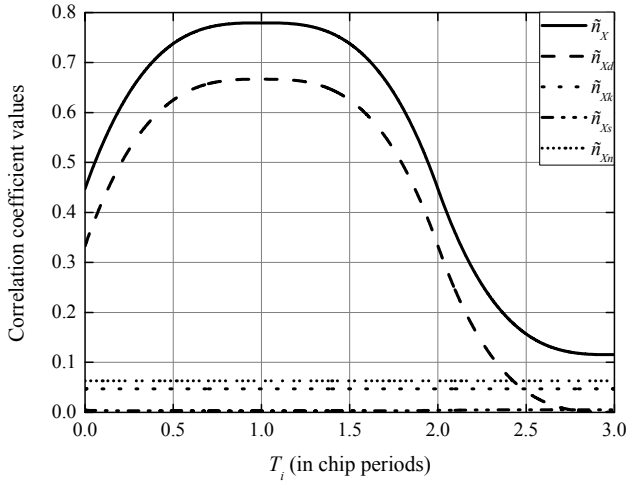


**Fig. 2.** Autocorrelation coefficients as a function of the finger position (uniform PDP).

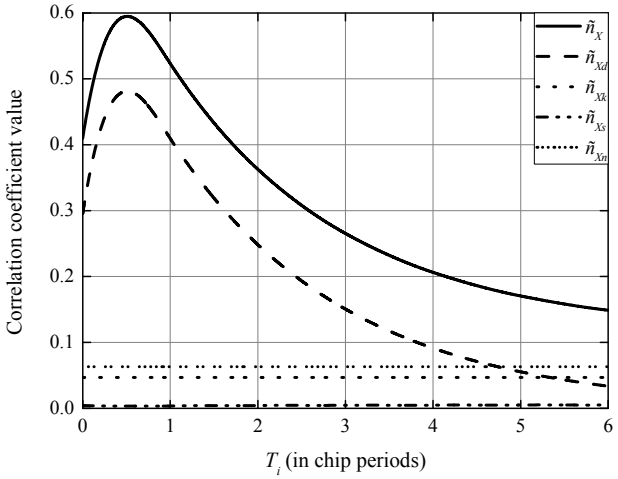


**Fig. 5.** Autocorrelation coefficients as a function of the finger position (exponential PDP).

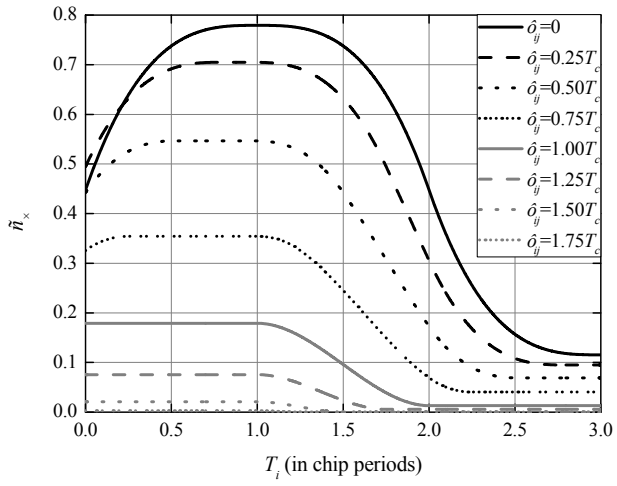


**Fig. 3.** Total signal correlation coefficients as a function of the finger position (uniform PDP).

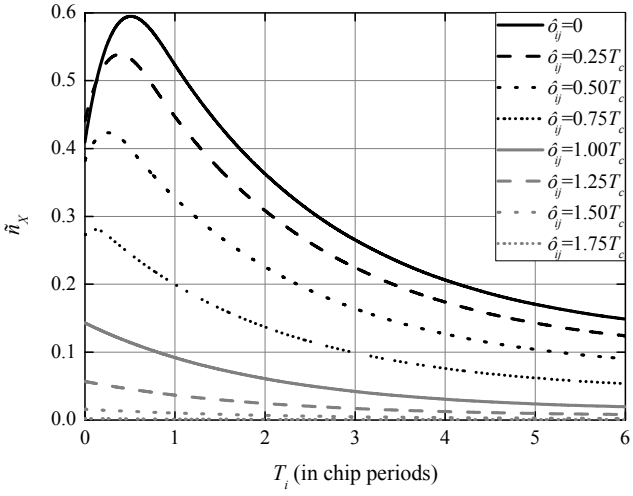


**Fig. 6.** Total signal correlation coefficients as a function of the finger position (exponential PDP).

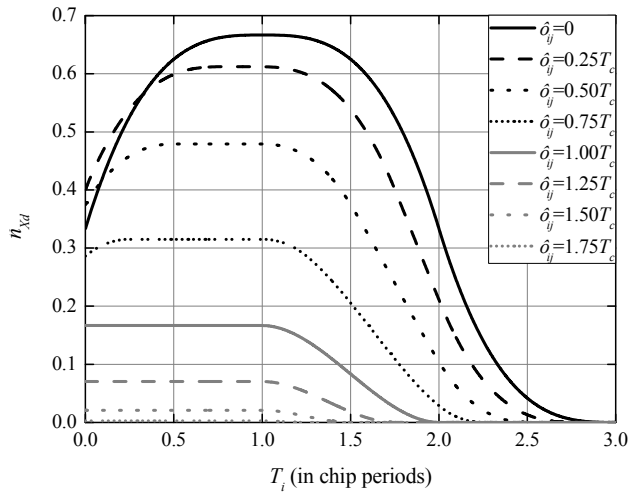


**Fig. 4.** Desired signal correlation coefficients as a function of the finger position (uniform PDP).

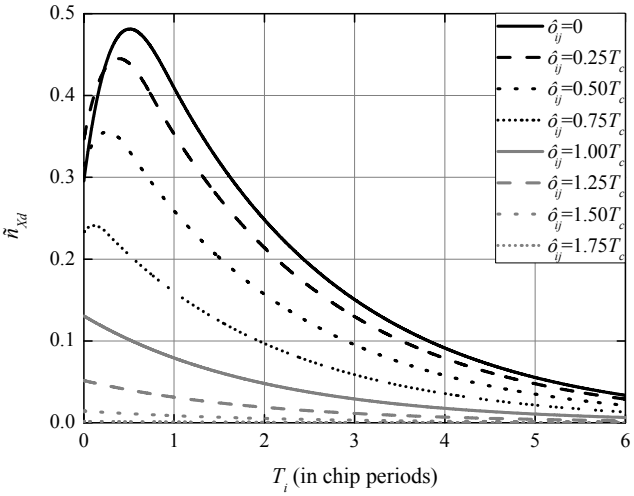


**Fig. 7.** Desired signal correlation coefficients as a function of the finger position (exponential PDP).

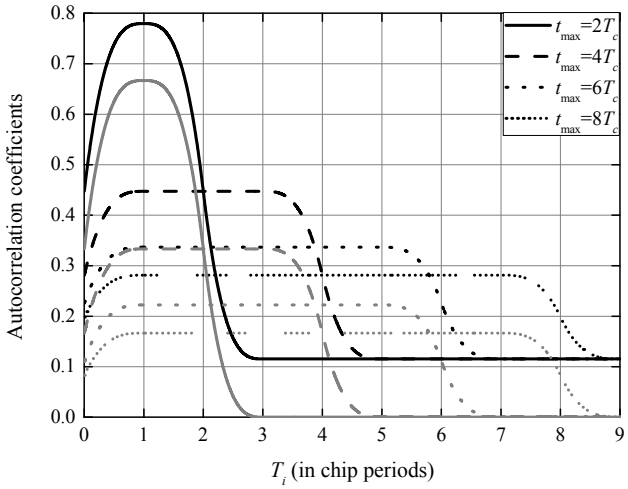


**Fig. 8.** Total (black line) and desired (gray line) signal autocorrelation coefficients for varied channel spread (uniform PDP).

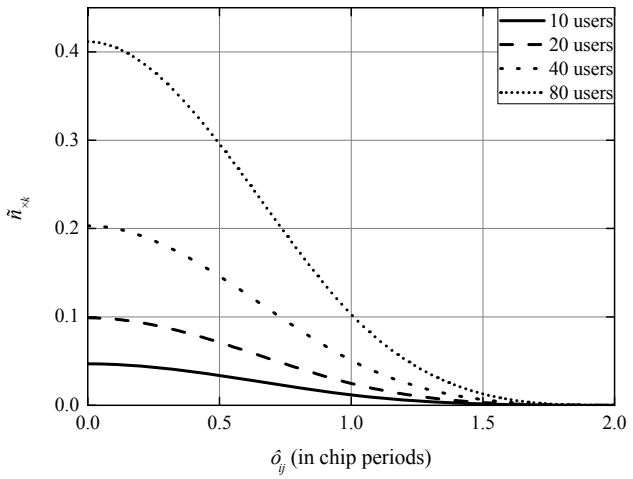


**Fig. 10.** Impact of finger spacing on the MUI correlation coefficient component for various number of users.

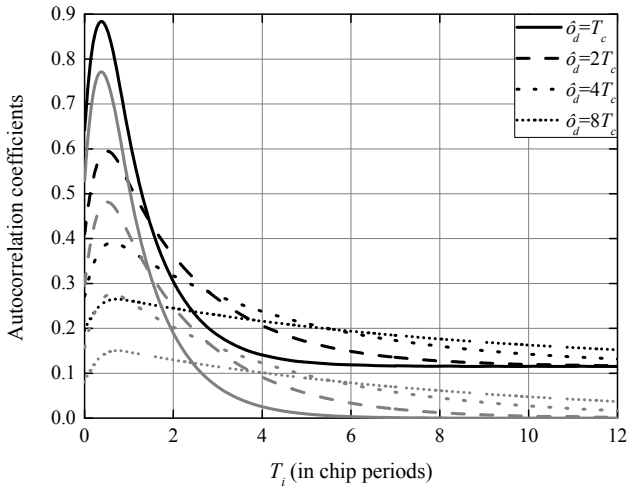


**Fig. 9.** Total (black line) and desired (gray line) signal autocorrelation coefficients for varied channel spread (exponential PDP).

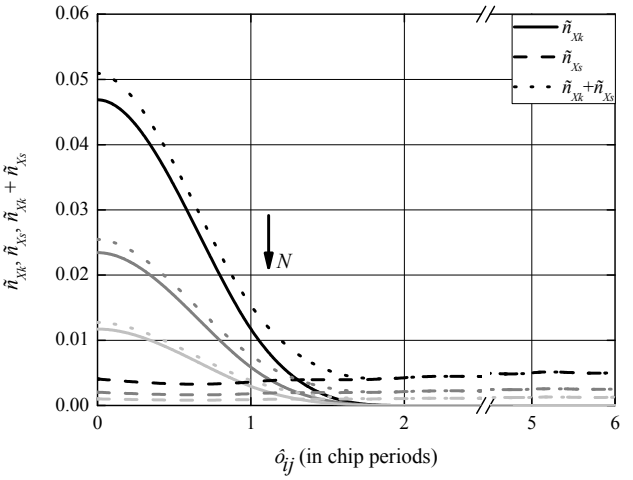


**Fig. 11.** MUI and ISI correlation coefficients versus finger spacing (black lines: $N$=256, dark gray lines: $N$=512, light gray lines: $N$=1024).

of this term in $\rho_X$; recall that $N>>1$ in a real DS/SS communication system [5]). In the uniform PDP case, the received energy of the desired signal resides up to $\tau_{max} + T_C$, as $T_i$ increases, $\rho_X$ is only due to noise. Increase in $\tau_{max}$ lowers the level of the curves; the curves are also practically constant over a wider range of $T_i$ values. In the exponential PDP channel, we further notice that the maxima of $\rho_X$ and $\rho_{Xd}$ slightly shift to the left as decay constant decreases.

Fig. 10 illustrates $\rho_{Xk}$ versus $\tau_{ij}$ for $N$=256 and various $K$ ($\rho_{Xk}$ does not depend on $T_i$, see (17)). Notice that the curves lower with $K$ (eq. (17) gives that $\rho_{Xk}$ is proportional to the number of users). As finger spacing increases, $\rho_{Xk}$ decreases. The term is practical negligible when finger spacing is greater than $1.5T_c$ (due to the time-limited rectangular shape of the pulses).

An example that shows the relationship between the correlation coefficients and $N$ follows. Fig. 11 illustrates $\rho_{Xk}$, $\rho_{Xs}$ ($\rho_{Xd}$ and $\rho_{Xn}$ does not depend on $N$, see (16) and (19)) and their sum versus $\tau_{ij}$ for $N$=256, 512 and 1024. Ten users and an exponential PDP with $\tau_d = 2T_C$ are considered. In $\rho_{Xs}$ curves, the first finger is placed at 0. Coefficients decrease with $N$. The MUI coefficient is inversely proportional to $N$, see (18). A similar dependence is expected for the ISI coefficient due to the insignificant contribution of the second term in (18); see also [11].

In Fig. 12, the autocorrelation coefficient of the ISI component is presented. System characteristics are as in the previous example. The low values of $\rho_{Xs}$ and their decrease with $N$ are shown. Notice that the curves slightly increase with $T_i$ and show a periodic variation with period almost equal to the chip period. This complicated nature of the ISI component results from the summation of infinite (in practice, of a limited number [11]) terms. A detailed analy-

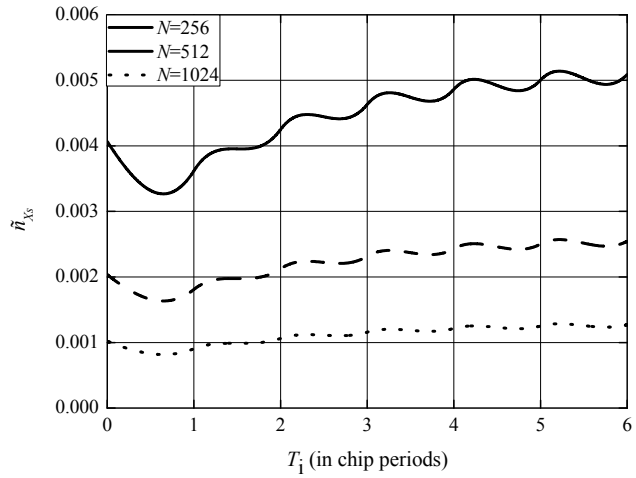


**Fig. 12.** Impact of finger spacing on the ISI autocorrelation coefficient component for different processing gains.

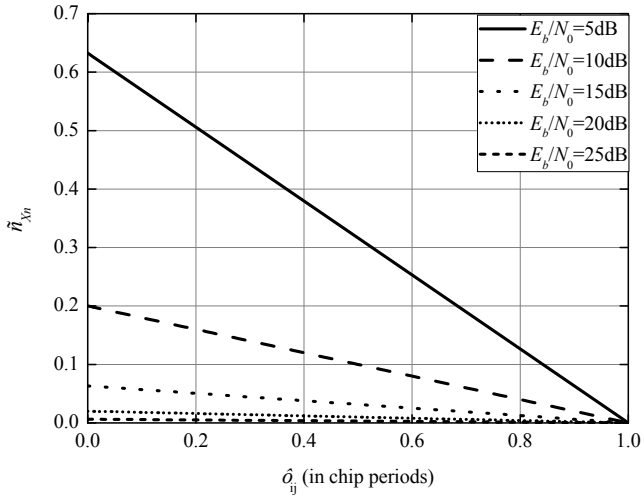


**Fig. 13.** Impact of finger spacing on the AWGN correlation coefficient component for varying $E_b/N_0$.

sis of this issue is beyond the scope of the paper due to the small contribution of the term in $\mathbf{C}^n$.

The AWGN correlation coefficient $\rho_{Xn}$ is linearly dependent to $N_0$, i.e. it is inversely proportional to the bit energy to noise power spectral density $E_b/N_0$, and depends on $\tau_{ij}$, see (19). Fig. 13 illustrates $\rho_{Xn}$ as a function of $\tau_{ij}$ for different values of $E_b/N_0$. The term becomes negligible for $E_b/N_0$> 20dB. As a result of the shape of the pulses, the relation between $\rho_{Xn}$ and $\tau_{ij}$ is linear and $\rho_{Xn} = 0$ for $T_i > T_c$.

## 4.2 A Low Computational Complexity Rake Receiver

In the previous subsection, we have noticed the similarities between the total and the desired signal correlation coefficients curves. Based on this, a low computational complexity finger placement criterion is proposed.

In [11], the fractionally spaced maximum power minimum correlation (MPMC) rake receiver has been proposed. The MPMC criterion was used for the optimization of fingers positions. This criterion was a multi-objective optimization problem [22], [23], based on the simultaneous maximization of the sum of squares of autocorrelation, i.e. the average received signal power in each finger and minimization of the sum of squares of cross-correlation between each pair of fingers. The criterion was defined as:

$$\text{find } \mathbf{T}: \max_{\mathbf{T}} F(\mathbf{T}) \qquad (24)$$

$$\text{subject to}: T_i \in \left[T_{i-1}^0, T_i^0\right], \quad i = 1,2..L \qquad (25)$$

where $T_0^0 = 0$ and $T_i^0 = g^{-1}\left[G(0) + (2i+1)/(2L+1)\right]$ for $i$=1,2..$L$. Functions $g^{-1}(t)$ and $G(t)$ are correspondingly the inverse and the antiderivative functions of $g(t)$. The objective function is the

$$F(\mathbf{T}) = \{f_1(\mathbf{T}), f_2(\mathbf{T})\} \qquad (26)$$

where:

$$f_1(\mathbf{T}) = \sum_{i=1}^{L} \mathrm{E}\left[\left|X(T_i)\right|^2\right]^2, \qquad (27)$$

$$f_2(\mathbf{T}) = \frac{1}{\sum_{i=1}^{L}\sum_{j=i+1}^{L} \mathrm{E}\left[X(T_i)X^*(T_j)\right]^2}. \qquad (28)$$

Based on the similarities of $\rho_X$ and $\rho_{Xd}$ curves, a Low Computational Complexity (LCC) MPMC criterion is proposed. This criterion is defined from (24)-(25), but the quantities $X(T)$ in (27)-(28) are replaced by $X_d(T)$, i.e. we use the elements of $\mathbf{C}^d$ instead of $\mathbf{C}$. The significant reduction in computational complexity is obvious (it decreases at least by 50% when $\rho_{Xs}$ is not considered; when the MPMC criterion considers this component the complexity reduction of the proposed algorithm is significantly greater).

In Tab. 1, the optimum finger positions calculated from the LCC-MPMC criterion are given. Receivers with one, two, three, and four fingers in uniform, with $t_{max}=2T_c$, and exponential, with $\tau_d = 2T_C$, PDP environments are considered. The results from the application of the MPMC criterion (see Tab. 1 in [11]) are in parentheses. We notice that the two criteria give similar results.

In Figs. 14-15, the bit error probability (BER) versus the bit energy to noise power spectral density is illustrated for the MPMC and the LCC-MPMC rake receivers and the cases presented in Tab. 1. In these examples, $K = 10$ and $N = 256$ (this choice has been made for comparison reasons with the results in [11]). We assume that the receivers have perfect knowledge of the chip waveform shaping filters in transmitter and receiver and that an accurate estimation of the channel impulse response of the desired user is also possible. The examples presented here show that receiver

| Fing. setting | | $T_1$ | $T_2$ | $T_3$ | $T_4$ |
|---|---|---|---|---|---|
| Unif. PDP | L=1 | 1.00(1.00) | - | - | - |
| | L=2 | 0.31(0.49) | 1.58(1.50) | - | - |
| | L=3 | 0.26(0.28) | 0.93(0.98) | 1.64(1.69) | - |
| | L=4 | 0.30(0.28) | 0.65(0.65) | 1.34(1.30) | 1.70(1.70) |
| Exp. PDP | L=1 | 0.51(0.51) | - | - | - |
| | L=2 | 0.44(0.43) | 1.83(1.82) | - | - |
| | L=3 | 0.38(0.36) | 1.32(1.30) | 2.35(2.32) | - |
| | L=4 | 0.33(0.31) | 1.01(1.00) | 1.77(1.74) | 2.64(2.64) |

**Tab. 1.** Proposed (optimum) finger allocation.

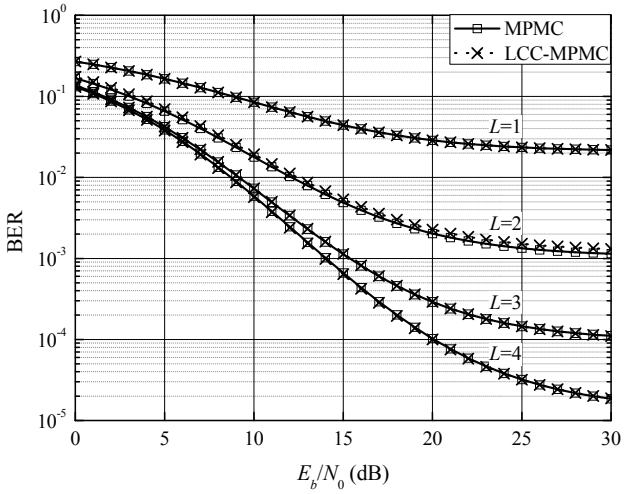


**Fig. 14.** BER performance of MPMC and LCC-MPMC rake in the uniform PDP environment.

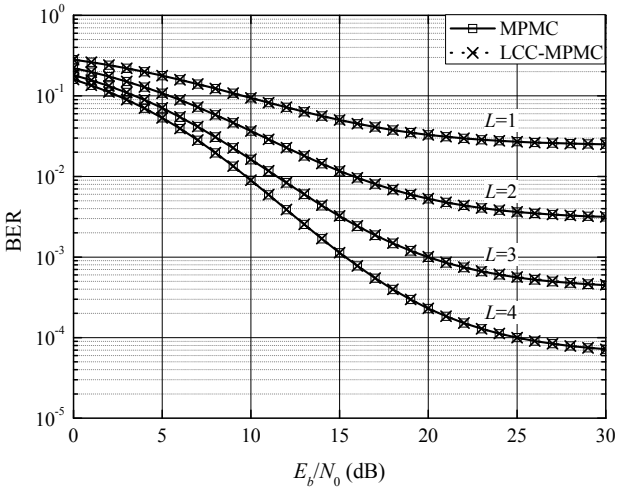


**Fig. 15.** BER performance of MPMC and LCC-MPMC rake in the exponential PDP environment.

performance is practically the same when finger placement is based on the LCC-MPMC instead of the MPMC criterion (a detailed analysis of receiver performance is beyond the scope of this paper). It has to be mentioned that the proposed criterion is not applicable in a practical receiver implementation (the direct calculation of the desired signal correlation coefficients is not possible). However, the accuracy of the derived results and the significant reduction in complexity makes the LLC-MPMC criterion a useful tool for the analysis and design of a wireless communication system.

# 5. Conclusions

In this paper, a detailed analysis of the relationship between finger placement and the correlation coefficients of rake combined signals was presented. The impact of system parameters such as the propagation channel characteristics, the number of users, the processing gain and the thermal noise power has also been discussed. Interesting conclusions have been derived. Our analysis allows a better understanding of the operation of rake receiver. As an application, a reduced complexity finger placement optimization criterion has been developed. The proposed receiver performs similarly to more complicated proposals in the literature. In order to fully exploit the advantages and practical applications of the presented analysis, its extension in more complicated wireless propagation environments under the consideration of non-rectangular pulses is considered as a future development.

# References

[1] LEE, J. S., MILLER, L. E. *CDMA Systems Engineering Handbook*. Boston: Artech House, 1998.

[2] HOLIŠ, J., PECHAČ, P. Simulation of UMTS capacity and quality of coverage in urban macro- and microcellular environment. *Radioengineering*, 2005, vol. 14, no. 4, p. 21-26.

[3] MALIK, W. Q., STEVENS, C. J., EDWARDS, D. J. Multipath effects in ultrawideband rake reception. *IEEE Transactions on Antennas and Propagation*, 2008, vol. 56, no. 2, p. 507-514.

[4] SABERINIA, E., TANG, J., TEWFIK, A. H., PARHI, K. K. Pulsed-OFDM modulation for ultrawideband communications. *IEEE Transactions on Vehicular Technology*, 2009, vol. 58, no. 2, p. 720-726.

[5] TACHIKAWA, K., (Ed.). *W-CDMA Mobile Communications System*. Chichester: John Wiley & Sons Ltd, 2002.

[6] PROAKIS, J. G., SALEHI, M. *Digital Communications*. 5th ed. New York: McGraw-Hill, 2007.

[7] KIM, K. J., KWON, S. Y., HONG, E. K., WHANG, K. C. Effect of tap spacing on the performance of direct-sequence spread spectrum RAKE receiver. *IEEE Transactions on Communications*, 2000, vol. 48, no. 6, p. 1029-1036.

[8] BOTTOMLEY, G. E., OTTOSON, T., WANG, P.-E. A generalized RAKE receiver for interference suppression. *IEEE Journal on Selected Areas in Communications*, 2000, vol. 18, no. 8, p. 1536-1545.

[9] SUI, H., MASRY, E., RAO, B. D. Chip-level DS-CDMA downlink interference suppression with optimized finger placement. *IEEE Transactions on Signal Processing*, 2006, vol. 54, no. 10, p. 3908-3921.

[10] GEZICI, S., CHIANG, M., POOR, H. V., KOBAYASHI, H. Optimal and suboptimal finger selection algorithms for MMSE rake receivers in impulse radio ultra-wideband systems. *EURASIP Journal on Wireless Communications and Networking*, 2006, 10 pages. DOI: 10.1155/WCN/2006/84249.

[11] BALTZIS, K. B., SAHALOS, J. N. A novel RAKE receiver design for wideband communications. *Wireless Personal Communications*, 2007, vol. 43, no. 4, p. 1603-1624.

[12] HE, J., SALEHI, M. A new finger placement algorithm for the generalized RAKE receiver. In *Proceedings of the 42nd Annual Conference on Information Sciences and Systems (CISS 2008)*. Princeton (USA), 2008, p. 335-340.

[13] BALTZIS, K. B. An efficient finger allocation method for the maximum likelihood RAKE receiver. *Radioengineering*, 2008, vol. 17, no. 4, p. 45-50.

[14] JERUCHIM, M. C., BALABAN, P., SHANMUGAN, K. S. *Simulation of Communications Systems: Modeling, Methodology and Techniques*. 2nd ed. New York: Kluwer Academic/Plenum Publishers, 2000.

[15] CHOI, S., ALOUINI, M. –S., QARAQE, K. A. Finger management schemes for RAKE receivers with a minimum call drop criterion. *IEEE Transactions on Communications*, 2009, vol. 57, no. 2, p. 348-352.

[16] DOĞAN, H., PANAYIRCI, E., ÇIRPAN, H. A., FLEURY, B. E. MAP channel-estimation-based PIC receiver for downlink MC-CDMA systems. *EURASIP Journal on Wireless Communications and Networking*, 2008, 9 pages. DOI: 10.1155/2008/570624.

[17] SEPTIER, F., DELIGNON, Y., MENHAJ-RIVENQ, A., GARNIER, C. Non-pilot-aided sequential Monte Carlo method to joint signal, phase noise, and frequency offset estimation in multicarrier systems. *EURASIP Journal on Advances in Signal Processing*, 2008, 14 pages. DOI: 10.1155/2008/612929.

[18] OLIVEIRA, L. D., CIRIACO, F., ABRÃO, T., JESZENSKY, P. J. E. Local search multiuser detection. *AEU International Journal of Electronics and Communications*, 2009, vol. 63, no. 4, p. 259-270.

[19] KADDOUM, G., ROVIRAS, D., CHARGÈ, P., FOURNIER-PRUNARET, D. Robust synchronization for asynchronous multi-user chaos-based DS-CDMA. *Signal Processing*, 2009, vol. 89, no. 5, p. 807-818.

[20] LI, X. J., CHONG, P. H. J. Performance investigation of CDMA/PRMA with imperfect power control in TDD cellular systems. *Wireless Personal Communications*, 2009, 12 pages. DOI: 10.1007/s11277-009-9729-9.

[21] DONG, X., BEAULIEU, N. C. Optimal maximal ratio-combining with correlated diversity. *IEEE Communication Letters*, 2002, vol. 6, no. 1, p. 22-24.

[22] BRANKE, J., DEB, K., MIETTINEN, K., SŁOWIŃSKI, R. (Eds.) *Multiobjective Optimization: Interactive and Evolutionary Approaches*. Berlin: Springer-Verlag: 2008.

[23] MARLER, T., ARORA, J. S. *Multi-Objective Optimization: Concepts and Methods in Engineering*. Saarbrucken: VDM Verlag, 2009.

## About Author...

**Konstantinos B. BALTZIS** was born in Thessaloniki, Greece. He received his B.Sc. degree in physics in 1996, his M.Sc. degree in electronics and communications in 1999, and his PhD degree in communication engineering in 2005, all from the Aristotle University of Thessaloniki (AUTh), Greece. He is a member of the permanent research staff of the RadioCommunications Laboratory of AUTh and works as a part time assistant professor in the Department of Automation at the Technological Educational Institute of Thessaloniki. He is also a teaching staff member in the Program of Postgraduate Studies in Electronic Physics of AUTh. His research interests include spread spectrum systems, wireless networks, radiowave propagation, microwave devices, optimization techniques and education.